ELECTRONIC SUPPLEMENTARY INFORMATION

Table of Contents

I. Dependence of photocurrent on oxygenate concentration

To view the influence of oxygenate concentration on WO_3 photocurrent, a CA scan at +1.2 V

SCE was conducted with a starting electrolyte of 0.33 M H_2SO_4. The oxygenate concentration

was incrementally increased by adding small quantities of concentrated oxygenate solution. After

each addition, the solution was thoroughly mixed and the photocurrent allowed to stabilize for 60

s before its value was recorded. During this experiment the potential of the WO_3 photoanode was

held at 1.2 V versus the saturated calomel electrode (SCE) while the photocurrent was recorded

as a function of glucose and methanol concentrations (Fig. S1). At low concentrations, the

photocurrent increases sharply with oxygenate concentration, which is most likely indicative of

diffusion-limited behaviour. In this regime, the photocurrent is suppressed compared to the

maximum current because the rate of oxygenate diffusion is less than the flux of photo-generated

holes to the WO_3 surface. Under these conditions, a fraction of holes reaching the surface are

likely to be consumed by the less favorable oxygen evolution reaction (OER) or sulfate oxidation

side reactions. At higher concentrations, a second regime is observed where the photocurrent

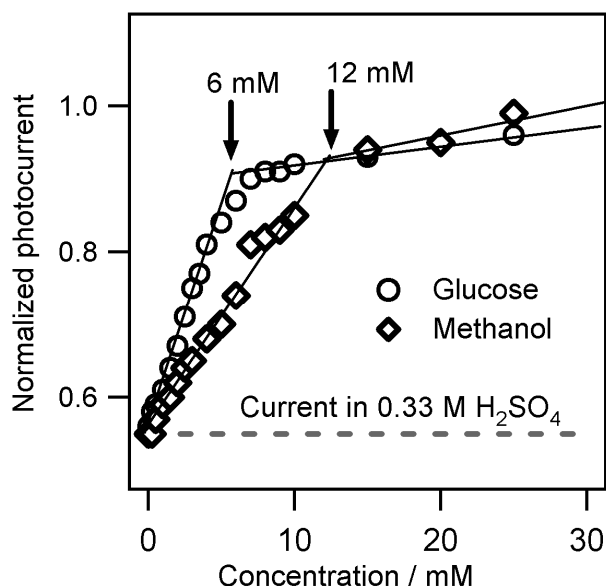levels off and is limited by the flux of holes to the WO_3 surface.

Figure S1. Photocurrent measured for WO_3 photoelectrode at 1.2 V SCE in methanol and glucose-containing 0.33 M H_2SO_4 electrolytes as a function of oxygenate concentration. Photocurrents were normalized to the photocurrent recorded at a glucose concentration of 50 mM.

From the distinct change in the slopes of the curves in Figure S1, the boundary between the

diffusion-limited and light absorption-limited regimes can be approximated. Importantly, the

concentration at which mass transport becomes limiting for glucose (~ 6 mM) is significantly

lower than that for methanol (~12 mM) under the conditions tested. This is surprising given the

larger diffusion coefficient for methanol (1.3×10^{-4} m^2/s) than glucose (8.8×10^{-5} m^2/s),[1] but may

be explained by the difference in electrons transferred per glucose molecule (maximum of 24 e⁻)

compared to methanol (maximum of 6 e⁻). The higher ratio of electrons per reactant molecule in

glucose allows for larger photocurrents than methanol under diffusion limiting conditions.

II. Surface analysis of WO$_3$ photoelectrodes following photo-oxidation of glucose

Figure 6 of the main article gives indirect evidence that carbon deposition does not take place at the WO$_3$ photoelectrode since the photocurrent of the WO$_3$-based tandem cell device in the 0.1 M glucose electrolyte was observed to be constant over the course of 40 minutes of operation. If carbon were gradually deposited and built-up on the photoelectrode surface during operation in the glucose-containing electrolyte, one would expect that the active WO$_3$ sites would gradually be blocked from the electrolyte, resulting in a decrease in the measured photocurrent (reaction rate).

In order to further investigate the possibility of carbon deposition, X-ray photoelectron spectroscopy (XPS) measurements were carried out to directly quantify the amount of carbon on the WO$_3$ surface. For this experiment, two identical and pristine WO$_3$ photoanodes were subjected to a one-hour long chronoamperometry (CA) measurement with an applied potential of +1.2 V vs. SCE. The CA for the first electrode was performed in 0.33 M H$_2$SO$_4$, while the CA for the second electrode was carried out in 0.33 M H$_2$SO$_4$ + 0. 1 M glucose, identical to that used for tandem cell tests in the main article. Before and after CA measurements (Figure S2a), XPS was used to monitor changes in the atomic ratio of carbon to tungsten on the WO$_3$ surface. Since XPS is a surface sensitive technique, an increase in the build-up of carbon on the surface during glucose oxidation would be expected to result in a significant increase in the measured (C/W) atomic ratio. However, Figure S2b shows that the (C/W) atomic ratio actually decreases slightly after the CA measurements, most likely because the electrochemical measurement removed some adventitious carbon that was originally present on the WO$_3$ surface. The finding of a slight decrease in the atomic (C/W) ratio provides strong evidence that carbon was not deposited on the WO$_3$ photoelectrode operating in the glucose-containing electrolyte. Equally important is the

fact that the WO_3 photocurrent in glucose never decreased over the course of the CA measurement, as was already noted for operation of the tandem cell device in the main article.
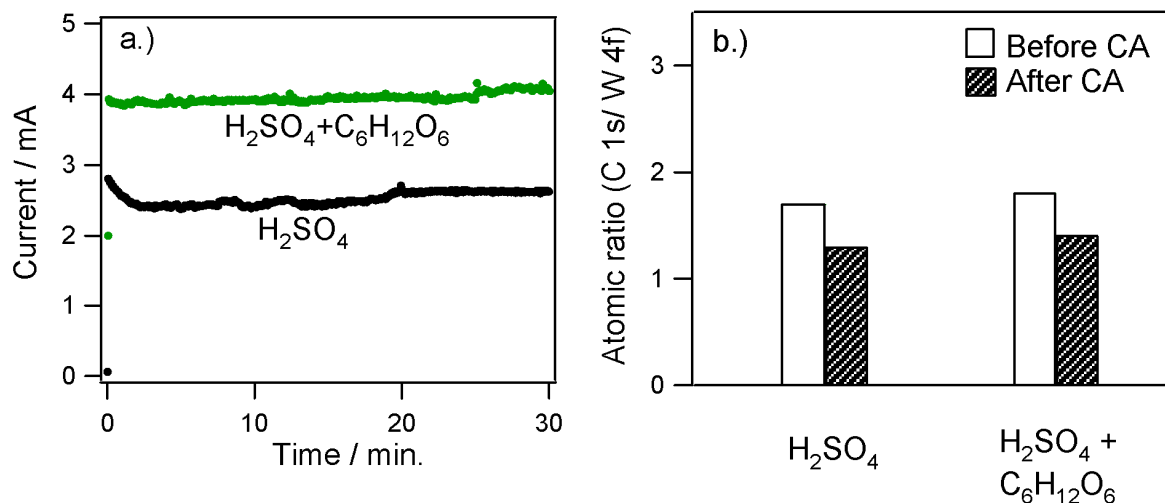

Figure S2. a.) CA measurements for WO_3 photoelectrodes with an applied potential of +1.2 V vs. SCE in 0.33 M H_2SO_4 and 0.33 M H_2SO_4+ 0.1 M $C_6H_{12}O_6$. b.) Atomic ratios of (C 1s/ W 4f) for WO_3 photoanodes determined by XPS following the CA measurements in a.).

III. Prediction of Tandem Cell performance

As previously demonstrated,[2,3] a useful method for predicting and evaluating the performance of a PEC device is to superimpose the current-voltage (JV) curves of individual components on a common voltage scale. In this work, each component of the integrated $WO_3|CdTe|WC$ device was wired independently, allowing for measurement of the JV characteristics of individual components or of the integrated device. In Figure S3a, the JV (or LSV) curves measured for each of the individual components of the $WO_3|CdTe|WC$ tandem device in 0.33 M H_2SO_4 are plotted with respect to the normal hydrogen electrode (NHE). Figure S3a was constructed by positioning the JV curve for the filtered CdTe layer such that its short-circuit operating point (V_{cell}=0.0 V)

intersected the WC LSV curve at the potential where the current through the WC counter electrode was equal to the J_{sc} of the CdTe layer. The predicted short-circuit current density ($J_{sc,device}$) and potential ($V_{sc,device}$) of the device are given by the intersection of the WO_3 and CdTe JV performance curves. Since J_{sc} is directly proportional to $H_{2(g)}$ production, Figure S3a shows that the H_2 production rate of the tandem device in the glucose-containing solution is expected to be nearly two times larger than that in H_2SO_4 alone. $V_{sc,device}$ is a useful operating parameter to monitor because it represents the common operating potential/voltage of the back contact of the photoanode and front contact of the PV component in the integrated device. Thus, when $V_{sc,device}$ and $J_{sc,device}$ are measured simultaneously during device operation, the performance of individual components can be evaluated during operation of the integrated device.[3]

To test the predictions of Figure S3a, the $J_{sc,device}$ and $V_{sc,device}$ of the WO_3|CdTe|WC tandem cell were monitored during 30 minutes of device operation under illumination by a Xe arc lamp at 100 mW cm^{-2}. This measurement was performed in 0.33 M H_2SO_4 (black curves) and 0.1 M glucose in 0.33 M H_2SO_4 (green curves), with the results provided in Figures S3b and S3c showing excellent quantitative agreement with those predicted in Figure S3a. Note that the steady state $J_{sc,device}$ values in both solutions are significantly lower than those achieved during testing under outdoor solar illumination (Fig. 6 of the main article). The lower $J_{sc,device}$ under artificial illumination is due to a deficiency in UV/blue portion photons for the filtered Xe Arc lamp compared to the actual AM 1.5 spectrum.
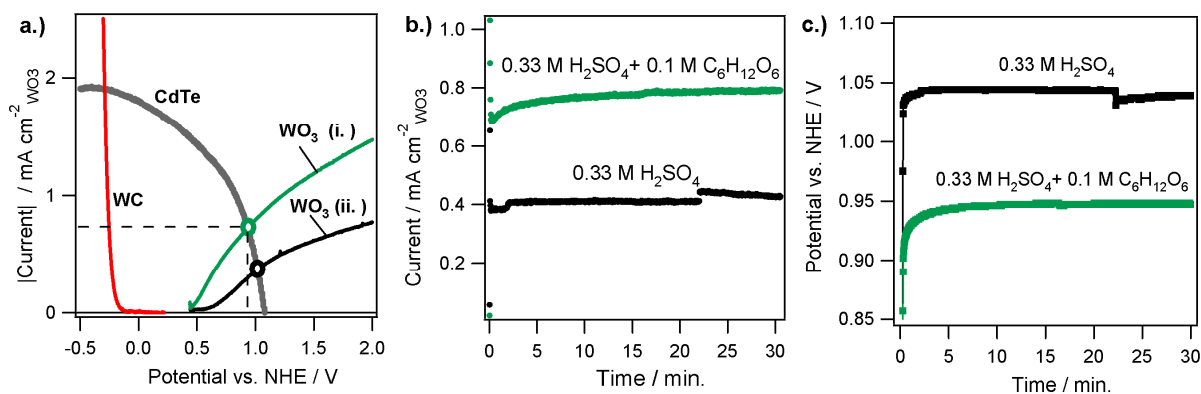
Figure S3. a.) Superposition of LSV and JV curves measured independently for each of the three major components (WO_3 , CdTe, and WC) of the tandem cell device shown in Figure 5 of the main article. LSV curves for the WO_3 photoanode are provided for 0.1 M $C_6H_{12}O_6$ +0.33 M H_2SO_4 (curve **i.**) and 0.33 M H_2SO_4(curve **ii.**). The open circles at the intersections of the CdTe JV curve with the WO_3 LSV curves gives the predicted short-circuit operating points ($J_{sc,device}$ and $V_{sc,device}$) for the integrated WO_3|CdTe|WC device. b.) Short circuit current densities and potentials of the WO_3|CdTe|WC tandem device simultaneously recorded for 30 minutes under illumination by a Xe arc lamp (100 mW cm^{-2}).

References

1. "Diffusion Coefficients in Liquids at Infinite Dilution" in *Internet Version of* CRC handbook of chemistry and physics, eds. W. M. Haynes and D. R. Lide, Taylor and Francis Group, LLC, 91st Edition, 2011.

2. E. L. Miller, B. Marsen, D. Paluselli and R. Rocheleau, *Electrochem. Solid-State Lett.*, 2005, **8**, A247-A249.

3. D. V. Esposito, O. Y. Goue, K. D. Dobson, B. E. McCandless, J. G. Chen and R. W. Birkmire, *Rev. Sci. Instrum.*, 2009, **80**.